Synchronization of chaotic oscillations in doped fiber ring lasers

Clifford Tureman Lewis,* Henry D. I. Abarbanel,† Matthew B. Kennel,‡ Michael Buhl,§ and Lucas Illing‖
Institute for Nonlinear Science, University of California, San Diego, La Jolla, California 92093-0402
(Received 20 July 1999; revised manuscript received 15 August 2000; published 22 December 2000)

The synchronization of chaotic rare-earth-doped fiber ring lasers is analyzed. The lasers are first coupled by transmitting a fraction c of the circulating electric field in the transmitter and injecting it into the optical cavity of the receiver. A coupling strategy which relies on modulation of the intensity of the light alone is also examined. Synchronization is studied as a function of the coupling strength, and we see excellent synchronization, even with very small c. We prove that in an open loop configuration ($c=1$) synchronization is guaranteed due to the particular structure of our equations and of the injection method we use. The generalized synchronization of these model lasers is examined when there is parameter mismatch between the transmitter and receiver lasers. The synchronization is found to be insensitive to a wide range of mismatch in laser parameters, but it is sensitive to other parameters, in particular those associated with the phase and the polarization of the circulating electric field. Communicating information between the transmitter and receiver lasers is also addressed. We investigate a scheme for modulating information onto the chaotic electric field and then demodulating and detecting the information embedded in the chaotic signal passed down the communications channel. We show full recovery with very low error for a wide range of coupling strengths.

DOI: 10.1103/PhysRevE.63.016215 PACS number(s): 05.45.Xt, 05.45.Vx, 42.65.Sf, 42.55.Wd

I. INTRODUCTION

Synchronization of chaotic oscillators is a phenomenon found quite often in physical and biological systems. The idea that chaotic systems could synchronize their motions was suggested some time ago by Fujisaka and Yamada [1] and independently by Afraimovich, Rabinovich and Verichev [2]. An early investigation of synchronization in neural networks [3] explored application in a wider arena.

The idea was again independently proposed and then experimentally explored by Pecora and Carroll [4]. The latter authors also suggested that the use of synchronized chaotic oscillators for communications would be of some interest. The work of Pecora and Carroll led to the investigation of a wide variety of synchronized chaotic systems [5] including close relatives of those we discuss in this paper.

In this paper we explore the synchronization properties of the models we have built for rare-earth-doped fiber ring lasers (DFRLs) based on previous work done by us and our collaborators [6–9]. Our plan here is to use two such model lasers connecting them by transmitting the electric field $\mathbf{E}_T$ circulating in one laser (the transmitter) to a second identical laser (the receiver). Into the optical cavity of the receiver laser we re-inject a fraction $(1-c)\mathbf{E}_R$ of the receiver field $\mathbf{E}_R$ and also add a fraction $c\mathbf{E}_T$ of the field arriving from the first laser. The net field entering the receiver laser is then $c\mathbf{E}_T+(1-c)\mathbf{E}_R$. When the lasers are synchronized so that $\mathbf{E}_R=\mathbf{E}_T$, then the combination $c\mathbf{E}_T+(1-c)\mathbf{E}_R$ is independent of c and equal to the field in either laser. As we vary c, we change the precise combination of transmitter field and receiver field which is seen at the receiver.

We investigate the synchronization both for identical transmitter and receiver, and then for lasers which have various parameter mismatches including the gain and pumping of the active medium, their polarization characteristics, and their ring length. The synchronization is quite robust for mismatches in gain and pumping power, but it is very sensitive to mismatches in polarization or phase characteristics of the transmitter and receiver. Because of this sensitivity, we investigate another coupling strategy which uses only the intensity of the circulating electric fields to connect the transmitter and receiver. This is shown to be a potentially viable method of synchronizing the lasers, and an example of communicating using amplitude modulation of the transmitter intensity is investigated.

Many of the papers on synchronization of chaotic systems have dealt with applications to communications. While we are focused here on the use of doped fiber ring lasers, the principles associated with synchronization and communication are shared by earlier investigations, in particular at $c=1$ by the methods of Rulkov and Volkovskii [10] and those of Kocarev and Parlitz [11].

The attraction of using chaotic signals as the carriers of information comes from their potentially efficient use of channel bandwidth as well as the low cost and power efficiency of some chaotic transmitters and receivers [12]. There has also been much discussion of the security of communications systems based on chaotic carriers. The security of any such system depends on the details of the modulation methods used, not on the perception that the carrier is complex or temporally irregular. Whether any given modulation/demodulation strategy is secure needs to be determined

*Also at Department of Physics, University of California, San Diego. Email address: ctl@ucsd.edu
†Also at Department of Physics, and Marine Physical Laboratory, Scripps Institution of Oceanography, University of California, San Diego. Email address: hdia@jacobi.ucsd.edu
‡Email address: mkennel@ucsd.edu
§Also at Department of Physics, University of California, San Diego. Email address: mbuhl@click.ucsd.edu
‖Also at Department of Physics, University of California, San Diego. Email address: lilling@ucsd.edu

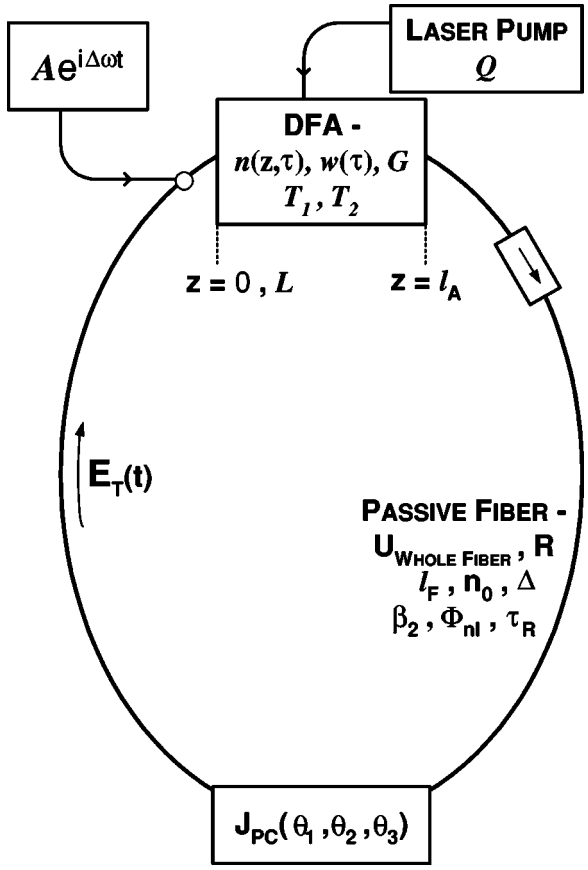

FIG. 1. A schematic diagram showing the relevant location of the parameters we consider in our model of coupled rare-earth-doped fiber lasers.

by a rigorous cryptographic analysis, and in this paper we do not discuss this issue or attempt to provide such an analysis.

II. EQUATIONS FOR AN INDIVIDUAL DFRL

We use the model introduced in [6]. The doped fiber ring laser (DFRL) we consider contains an optical amplifier composed of erbium-doped single-mode fiber of length l_A, whose active atoms are pumped by an external laser diode source. Connecting the output of this active section to its input is a piece of passive fiber of length l_F. In the passive fiber is an isolator which guarantees the direction of flow of light, a polarization controller, and a location where external light of given amplitude and frequency ω_I can be injected into the fiber. The total length of the fiber cavity is $L=l_A+l_F$. The general locations of the relevant parameters for each laser is shown schematically in Fig. 1.

Even though the erbium-doped fiber ring laser (EDFRL) is *multimode*, meaning there are many longitudinal modes being amplified inside the cavity, the dynamics of the ring laser can be described in terms of two orthogonally polarized supermodes [13]. Since the amplitude fluctuations of the amplitude of these supermodes is much slower than the optical frequency, it is common to model these electric fields amplitudes $\mathbf{E}(z,t)$ as the envelope $\mathcal{E}(z,t)$ of the optical plane wave of frequency ω_0, $\mathbf{E}(z,t)=\mathcal{E}(z,t)e^{i(k_0 z-\omega_0 t)}$ where $\omega_0=k_0c/n$ [14]. The dynamics of $\mathcal{E}(z,t)$ consists

• of linear birefringence of magnitude

$$\Delta=n_0(n_x-n_y), \tag{1}$$

where n_x and n_y are the indices of refraction along the principal axes of the fiber, and $n_0=(n_x+n_y)/2$,

• of group velocity dispersion (GVD) which comes from second order variations in frequency of the linear dispersion relation of the fiber,

• of contributions to the polarization of the medium associated with the population inversion of the atomic levels, and

• of nonlinear polarization effects associated with the Kerr term cubic in electric field strength.

With these effects included, our equations for the propagation of the electric field envelope $\mathcal{E}=(\mathcal{E}_x,\mathcal{E}_y)$ in the active medium $0\leqslant z\leqslant l_A$ become, in retarded coordinates $z=z$, $\tau=t-z/v_g$ with v_g is the group velocity of the waves,

$$\frac{\partial\mathcal{E}_{x,y}(z,\tau)}{\partial z}=gn(\tau)\mathcal{E}_{x,y}+\mathbf{L}_{x,y}\mathcal{E}_{x,y}+\mathbf{N}_{x,y}\mathcal{E}_{x,y}. \tag{2}$$

L contains the linear parts of the propagation operator excluding gain, and **N** is the Kerr nonlinearity. The linear operator **L**, including birefringence, GVD and gain dispersion, is most naturally represented in the Fourier domain:

$$\mathbf{L}_{x,y}=\pm\frac{ik_0(n_x-n_y)}{2n_0}\mp\frac{\Delta}{n_0c}i\omega-\frac{i}{2}\beta_2\omega^2-\frac{gn(\tau)\omega^2T_2^2}{1+\omega^2T_2^2} \tag{3}$$

with ω the signal angular frequency. The first term in $\mathbf{L}_{x,y}$ only results in an overall arbitrary phase shift for the two polarizations, which can be absorbed without loss of generality into the parametrization of the passive section described below. The term linear in ω represents linear birefringence; the next term, quadratic in ω, is the group velocity dispersion. The last term is associated with the gain curve, and arises from the fact that the center frequency of the line $\omega=0$ (ω_0) is amplified more strongly than frequencies on either side of the line. The nonlinear operators are

$$\mathbf{N}_x\mathcal{E}_x=i\chi_3\{(|\mathcal{E}_x(z,\tau)|^2+\tfrac{2}{3}|\mathcal{E}_y(z,\tau)|^2)\mathcal{E}_x(z,\tau)+\tfrac{1}{3}\mathcal{E}_x^*(z,\tau)\mathcal{E}_y(z,\tau)^2\}, \tag{4}$$

$$\mathbf{N}_y\mathcal{E}_y=i\chi_3\{(|\mathcal{E}_y(z,\tau)|^2+\tfrac{2}{3}|\mathcal{E}_x(z,\tau)|^2)\mathcal{E}_y(z,\tau)+\tfrac{1}{3}\mathcal{E}_y^*(z,\tau)\mathcal{E}_x(z,\tau)^2\}. \tag{5}$$

The physical implication of this third-order nonlinearity is most easily characterized by the non-dimensional phase shift Φ_{nl} experienced by an $\mathcal{E}$ field as it passes through the fiber given by [15]

$$\Phi_{nl}=\frac{\chi_3\pi L}{\lambda}(P_a+2P_b), \tag{6}$$

where P_a,P_b are the optical powers in the parallel and perpendicular directions. We parametrize our simulations by

Φ_{nl} and vary its value to tune in a desired amount of optical nonlinearity. Physically this could be interpreted as changing various parameters such as active medium pumping, which would increase the optical power, or changing the value of the ring fiber length L.

These equations must be solved numerically to propagate the light from its entry into the doped fiber amplifier at $z=0$ to its exit at $z=l_A$, represented here by a propagation operator on the vector $\mathcal{E}=[\mathcal{E}_x,\mathcal{E}_y]$: $\mathcal{E}(z=l_A,t+l_A/v)=\mathsf{P}\{\mathcal{E}(z=0,t)\}$.

The polarization of the electric field in the ring is affected by the birefringence in the fiber arising from numerous small effects associated with imperfections in the fiber, strains, etc. Following [16] we write the net effect of the fiber on the polarization states of the field as a unitary Jones matrix which we call $\mathbf{U}_{\text{Whole Fiber}}$.

The overall propagation map including all the passive parts of the ring and external injection is

$$\mathcal{E}(t+\tau_R)=\mathcal{A}(t+\tau_R)e^{i(\omega_I-\omega_0)(t+\tau_R)} + (\mathbf{R}\mathbf{J}_{PC}\mathbf{U}_{\text{Whole Fiber}})\mathsf{P}\{\mathcal{E}(t)\}. \quad (7)$$

Reading from left to right the terms are external monochromatic injection, possibly polarization dependent attenuation, $\mathbf{R}=\text{diag}(R_x,R_y)$, the unitary Jones matrix for the polarization controller $\mathbf{J}_{PC}$, the matrix for the passive fiber, and the propagator through the active medium. This discrete-time map, a recursion relation between the field at a time t and at a time τ_R later, is one of the dynamical rules of our ring laser system. The other is the population inversion equation in its simplified form.

The physics of the atomic polarization in the active medium is governed by the usual Bloch equation for the population inversion at time τ and spatial location z:

$$\frac{\partial n(z,\tau)}{\partial\tau}=Q-\frac{1}{T_1}(n(z,\tau)+1)-\xi n(z,\tau)|\mathcal{E}(z,\tau)|^2, \quad (8)$$

with Q the pumping strength, T_1 the lifetime of the excited state (10 ms for a typical erbium-doped fiber) and ξ a constant relating to the optical cross section governing the transition rate between levels. Assuming g real, we can integrate Eq. (8) by $l_A^{-1}\int_0^{l_A}dz$ to arrive at the dynamics for the population inversion averaged over the entire active medium $w(\tau)=l_A^{-1}\int_0^{l_A}dz\,n(z,\tau)$:

$$\frac{dw(\tau)}{d\tau}=Q-\gamma(w(\tau)+1+(e^{2l_Agw(\tau)}-1)|\mathcal{E}(z=0,\tau)|^2), \quad (9)$$

where γ is the ratio of round trip time to excited state lifetime τ_R/T_1.

Potentially, there is a third dynamical equation associated with the evolution of the polarization of the medium through which the electric field passes. The relaxation timescale for the medium polarization is about a picosecond, which is much smaller than either the electric field envelope fluctuations (on the order of a nanosecond) or the population inversion relaxation time (on the order of a millisecond). As is normally done in modeling EDFRLs [13,18], this medium polarization equation is adiabatically eliminated and the resulting ''static'' polarization is used in the electric field envelope and population inversion equations. This type of laser is known as a ''class B'' laser.

We summarize the equations for use below as a map $\mathbf{M}_{\mathcal{E}}(w(\tau),\mathcal{E}(\tau))$ of the electric field from time t to time $t+\tau_R$ and a differential equation for the integrated population inversion:

$$\mathcal{E}(\tau+\tau_R)=\mathbf{M}_{\mathcal{E}}(w(\tau),\mathcal{E}(\tau)),$$

$$\frac{dw(\tau)}{d\tau}=Q-\gamma\{w(\tau)+1+|\mathcal{E}(\tau)|^2(e^{Gw(\tau)}-1)\}, \quad (10)$$

where the active medium specific overall gain term G is defined as $G=2l_Ag$.

The details of our numerical schemes are to be found in our earlier paper [6]. Straightforward integration of the partial differential equations at a resolution sufficient to capture complex sub-round trip dynamics as seen in experiment results in an algorithm which is far too slow. We implemented a scheme which can integrate a whole round trip at a time, combined with a buffering method to process the portion of the linear operator in the Fourier domain. Still, computation takes approximately 18 hours on a contemporary workstation to achieve equilibrium (500 000 round trips) on account of the very large difference in time scales between the fluorescence lifetime $T_1\approx 10$ ms associated with an erbium-doped fiber and the time resolution of our simulation $\delta t\approx 80$ ps, necessary to capture the high frequency dynamics seen in experiment and thus high-bandwidth communication.

Using this model, we reached several fundamental conclusions regarding the dynamics of a single EDFRL. We numerically demonstrated that an EDFRL *can* exhibit chaotic dynamics, however the cause of the chaos is not the nonlinearity inherent in the interaction of the population inversion and the optical field. The population inversion dynamics are just too slow ($\gamma\approx 10^{-5}$). Instead, we concluded that the chaos comes from the nonlinear interaction of the optical field with itself (optical Kerr effect). The largest (positive) Lyapunov exponent λ_L was numerically found to be linearly dependent upon the Kerr coefficient (χ_3, which is a component of Φ_{nl}). Other effects, such as linear birefringence and optically injected light of another frequency, were found to have no clear functional effect on λ_L. The values of the model parameters used for the group of simulations in this paper are listed in Table I, and are typical for the type of EDFRL we are simulating [17]. The model with these parameters produces chaotic waveforms with a $\lambda_L=(6.3\pm 0.3)\times 10^3\,\text{s}^{-1}$, which corresponds to a characteristic divergence time of about a tenth of a millisecond.

III. SYNCHRONIZATION OF TWO DFRL

We now construct a transmitter and receiver pair and couple their electric fields by an optical channel. First we examine the synchronization of two identical lasers. Next we

TABLE I. Typical parameters for the EDFRL model simulations.

Quantity	Symbol	Value
Linear birefringence	Δ	1.8×10^{-6}
Fiber index of refraction	n_0	1.45
External injection amplitude	A	0.0
Pump strength	Q	2.4×10^{-2}
Overall gain term	G	1.35×10^{-2}
Absorption coefficients	R_x, R_y	0.45, 0.449995
Polarization controller angles	$\theta_1, \theta_2, \theta_3$	0.5, 1.2, 1.5
Nonlinear phase shift	Φ_{nl}	1.5×10^{-2}
Round trip time	τ_R	200 ns
Excited state lifetime	T_1	10 ms
Polarization dephasing time	T_2	1 ps
GVD coefficient	β_2	$-20\,\mathrm{ps}^2/\mathrm{km}$
Active fiber length	l_A	20 m
Passive fiber length	l_F	20 m

investigate the robustness of this synchronization as the transmitter and receiver are mismatched in various combinations of the physical parameters of the model, and as noise is added in the communication channel between transmitter and receiver. This will lead us into considerations of generalized, rather than identical synchronization. Last, we propose an alternate coupling scheme and synchronization method constructed to avoid some of the experimental problems typically encountered with direct optical coupling.

A. Identical transmitter and receiver

In our study of the synchronization of two EDFRLs we have a transmitter laser with dynamical variables $\mathcal{E}_T(t)$ and $n_T(t)$ and a receiver laser with $\mathcal{E}_R(t)$ and $n_R(t)$. The two lasers are started in different initial conditions, allowed to run uncoupled for several hundred thousand round trip times to reach their asymptotic state. Coupling is then activated. The transmitter's field $\mathcal{E}_T(t)$ is then injected into the receiver laser multiplied by a factor c while the circulating electric field in the receiver is attenuated by a factor $1-c$, and both are optically recombined before entering the rare-earth-doped amplifier section of the laser ring. The nonlinear amplifying element receives $c\mathcal{E}_T(t)+(1-c)\mathcal{E}_R(t)$ as its input. When the transmitter and receiver are synchronized, so $\mathcal{E}_T(t)=\mathcal{E}_R(t)$, the linear combination $c\mathcal{E}_T(t)+(1-c)\mathcal{E}_R(t)$ $=\mathcal{E}_R(t)=\mathcal{E}_T(t)$ is a solution to the equations of motion for each laser. This setup is illustrated in Fig. 2. We note here than the optical field extracted from the transmitter is negligible with respect to the transmitter dynamics. This is because if the field is extracted in the weak continuous manner, the results are equivalent to slightly altering the attenuation factors R_x and R_y. This has little effect except to slightly change the mean optical intensity in the transmitter which does not alter the optical field dynamics substantially. This kind of coupling is experimentally achievable with standard fiber optic equipment.

The equations for this unidirectional coupling between the chaotic systems are for the *transmitter*

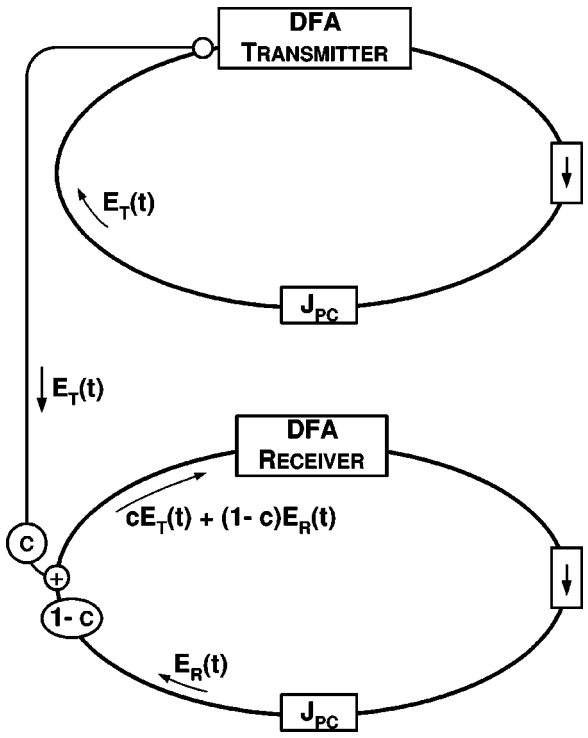

FIG. 2. The setup of coupled DFRLs. The electric field circulating in the transmitter laser is $\mathcal{E}_T(t)$. After it is transmitted through a channel to the receiver, a fraction $c\mathcal{E}_T(t)$ is injected into the input of the rare-earth-doped amplifier in the receiver ring. At the same time a fraction $(1-c)\mathcal{E}_R(t)$ of the field circulating in the receiver ring is added to it, so the net field injected into the amplifier input is $c\mathcal{E}_T(t)+(1-c)\mathcal{E}_R(t)$.

$$\mathcal{E}_T(\tau+\tau_R)=\mathbf{M}_{\mathcal{E}}(w_T(\tau),\mathcal{E}_T(\tau)),$$

$$\frac{dw_T(\tau)}{d\tau}=Q-\gamma\{w_T(\tau)+1+|\mathcal{E}_T(\tau)|^2(e^{Gw_T(\tau)}-1)\}, \tag{11}$$

and for the *receiver*

$$\mathcal{E}_R(\tau+\tau_R)=\mathbf{M}_{\mathcal{E}}(w_R(\tau),c\mathcal{E}_T(\tau)+(1-c)\mathcal{E}_R(\tau)),$$

$$\frac{dw_R(\tau)}{d\tau}=Q-\gamma\{w_R(\tau)+1+|c\mathcal{E}_T(\tau)+(1-c)\mathcal{E}_R(\tau)|^2(e^{Gw_R(\tau)}-1)\}. \tag{12}$$

When $c=0$, the lasers are uncoupled and run independently. If all of the physical parameters in the two laser subsystems are identical, the electric field in each laser visits the same attractor. $\mathcal{E}_T(t)$ and $\mathcal{E}_R(t)$ as well as $n_T(t)$ and $n_R(t)$ are uncorrelated due to the instabilities in the phase space of the system. As we increase c away from zero, we anticipate that for a certain minimum coupling, the lasers will asymptotically achieve identical synchronization, $\mathcal{E}_T(t)=\mathcal{E}_R(t)$, and $n_T(t)=n_R(t)$, even though the population inversions are not physically coupled. To exhibit this we run the two systems for the order of 10^4 round trips following their coupling. First, we ask after what time the quantity

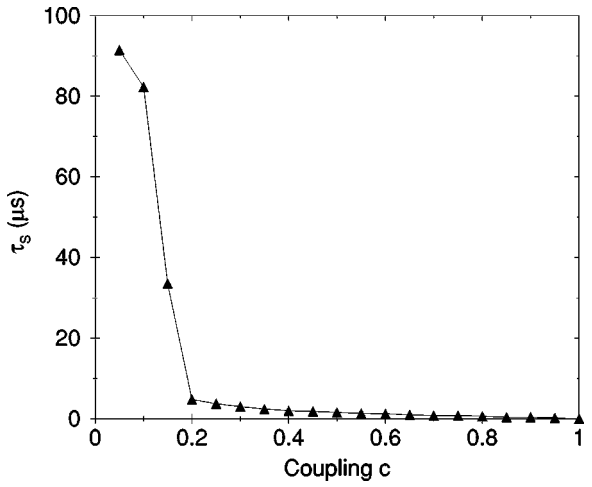

FIG. 3. Time to synchronization for identical DFRLs. The synchronization time τ_s is the time at which the amplitude synchronization error quantity $H_E(c,t)$ goes smaller than $\epsilon=10^{-2}$ and stays below for all larger times $t>\tau_s$. The value of τ_s is then averaged over 25 different initial conditions.

$$H_E(c,t)=\frac{|\mathcal{E}_T(t)-\mathcal{E}_R(c,t)|}{\langle|\mathcal{E}_T|\rangle_{\tau_R}} \tag{13}$$

becomes and remains less than some small number. The denominator is the average of $\mathcal{E}_T(t)$ taken over the round trip previous to coupling and is approximately constant from round trip to round trip, once the lasers pass the transient regime.

The time to synchronization τ_s is selected so at $t=\tau_s$ the synchronization error $H_E(c,t)$ becomes less than some small value ϵ, and then stays smaller than ϵ for all times $t>\tau_s$. Choosing $\epsilon=10^{-2}$, we plot τ_s in Fig. 3 as a function of c for $0\leqslant c\leqslant 1$. We see that for some values of $c\leqslant 0.1$, the lasers do synchronize, but it takes nearly 100 μs to come within ϵ. This is much longer than when $c\geqslant 0.2$, however, where synchronization sets in rapidly ($\tau_s\leqslant 5$ μs). This figure represents the average time to synchronization over 25 different initial conditions for each system, thus substantially reducing the effect of individual trajectory behavior. One lesson we can draw from Fig. 3 is that at $c=1$, which is open loop operation of the receiver, synchronization within ϵ sets in essentially instantaneously.

This τ_s is the time at which the synchronization error $H_E(c,t)$ falls below an arbitrary specified level, and reveals little about the extended temporal synchronization dynamics. We now examine the residual synchronization error $H_E(c,t)$ for large times after coupling. To assist us, we adopt the general unifying definition of synchronization proposed by Brown and Kocarev [19]. Their formalism states that two subsystems are synchronized with respect to the subsystem properties $g(x)$ and $g(y)$, if there is a time-independent function h, such that

$$||h[g(x),g(y)]||=0, \tag{14}$$

where $||\cdot||$ is some norm. The quantities $g(x)$ and $g(y)$ are completely general and can refer to any measurable property of the subsystem. The general form of the time-independent function h which we adopt here is

$$h[g(x),g(y)]\equiv\lim_{T\to\infty}\frac{1}{T}\int_t^{t+T}|g(x(s))-g(y(s))|ds. \tag{15}$$

For practical reasons, we must modify this statement somewhat, since numerically we can neither take $T\to\infty$, nor hope for $||h[g(x),g(y)]||$ to equal precisely zero, since we will reach the numerical limits of computation before that occurs.

To keep in the spirit of this definition, we let the coupled chaotic lasers run for K round trips after coupling, then calculate the RMS value of $H_E(c,t)$ over M additional round trips to examine the magnitude of the synchronization error for large times after coupling. This leads us to the synchronization error function

$$D_E(c)=\frac{1}{\mathcal{N}_E}\left(\int_{K\tau_R}^{(K+M)\tau_R}H_E^2(c,t)dt\right)^{1/2}. \tag{16}$$

The normalization factor $\mathcal{N}_E$ is the RMS average for the $c=0$ or uncoupled case

$$\mathcal{N}_E=\left(\int_{K\tau_R}^{(K+M)\tau_R}H_E^2(c=0,t)dt\right)^{1/2} \tag{17}$$

and is included to give us a tangible measure of the magnitude of the synchronization error at c versus the case of no coupling, $c=0$. In the work we report here we used $K=20\,000$ and $M=3000$.

Figure 4 displays the synchronization error function $\log_{10}[D_E(c)]$ versus c. We see a quite different picture of the synchronization here. Above we noted that for coupling as low as $c=0.1$, the lasers took a much longer time ($\approx$0.1 ms) than for higher coupling for $H_E(c,t)$ to become as small as ϵ. However, on the time scale of a few milliseconds, we see that with much smaller coupling the synchronization error $D_E(c)$ is less by many orders of magnitude. Note, however, that the error never exceeds a few parts in 10^7 for any c. Once the lasers synchronize at some c, they do so very accurately.

The apparent disagreement of these two plots leads us to the conclusion that there are two time scales of synchronization. There is an initial time scale ($t<1$ μs) with a rapid, short term convergence toward synchronization, then slower convergence rate for longer times ($t>1$ μs). For weaker coupling, the initial convergence of the lasers is not as large as for the stronger coupling case, since the amount of optical field from the transmitter being introduced into the receiver is proportional to the coupling strength. However, past this initial short time scale, the weaker coupling draws together the two lasers' trajectories at a faster rate than for the stronger coupling.

Figure 5 shows the rate of convergence plotted against coupling constant c, and we see that the magnitude of the convergence rate is maximal between $0.02\leqslant c\leqslant 0.04$. The coupling of the optical fields is linear in $\mathcal{E}_T(t)$ and $\mathcal{E}_R(t)$, so this complex synchronization behavior is not likely due to

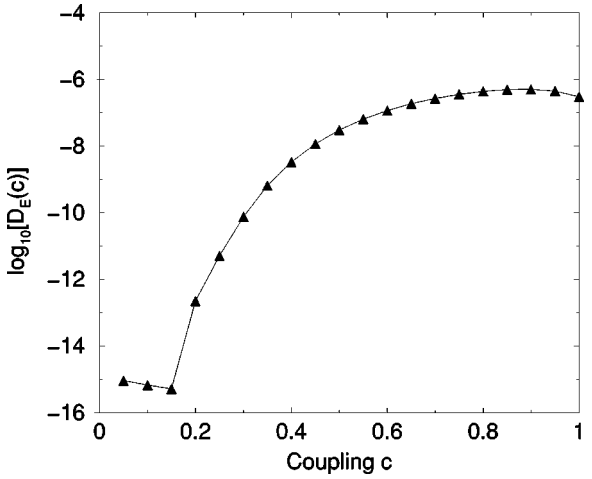

FIG. 4. Amplitude synchronization error $D_E(c)$ for identical DFRLs. The DFRLs are first coupled for $20\,000\tau_R$ and then the error term is averaged over an additional $3000\tau_R$. The result is then averaged over 25 initial conditions.

the optical field dynamics alone, therefore we look for explanations outside of the optical field variables. The other system variables are the population inversions $w_T(t)$ and $w_R(t)$. They cannot be directly coupled, being related only indirectly through the nonlinear relationship to their respective internal optical intensities [Eq. (9)]. In the transmitter, $w_T(t)$ is essentially constant because Erbium's fluorescence lifetime T_1 is so long ($T_1 \approx 10$ ms) that in the long-term asymptotic state of the laser, changes in $w_T(t)$ occur only on the order of 10^5 round trips. However, upon coupling, we cannot say the same for $w_R(t)$. There is always a rise in $w_R(t)$ immediately after coupling because when $0<c<1$, the intensity in the receiver laser just as the lasers are coupled is $|c\mathcal{E}_T|^2+|(1-c)\mathcal{E}_R|^2+2c(1-c)\mathbf{Re}(\mathcal{E}_T\cdot\mathcal{E}_R^*)$ averaged over a round trip, and the cross term averages to zero since the fields are initially uncorrelated. As $\langle|\mathcal{E}_T|^2\rangle$ and $\langle|\mathcal{E}_R|^2\rangle$ averaged over a round trip are equal, the average intensity initially entering the receiver's active medium will

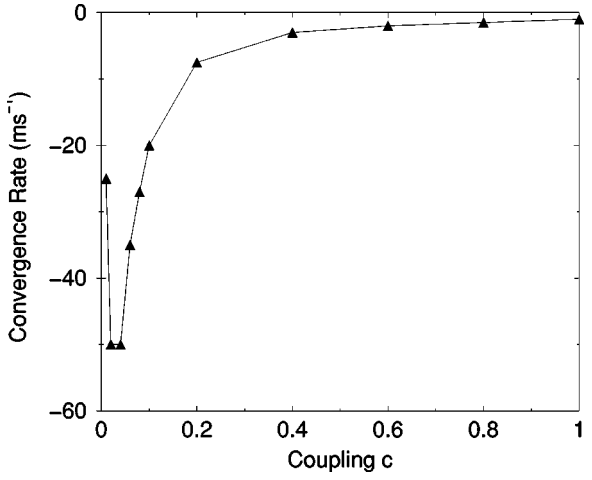

FIG. 5. Plot of the rate of convergence for the measure $D_E(c)$ for a range of coupling constants. The slope is calculated beginning after the initial convergence upon coupling. The lasers are identical.

be less than $\langle|\mathcal{E}_R|^2\rangle$ by a factor of $c^2+(1-c)^2$, where $1/2 \leqslant c^2+(1-c)^2 \leqslant 1$. This allows the pumping term to increase the receiver population inversion as the active medium sees a reduced intensity trying to stimulate transitions between lasing states.

This effect continues only as long as $\mathbf{Re}(\mathcal{E}_T\cdot\mathcal{E}_R^*) \ll |\mathcal{E}_T||\mathcal{E}_R|$. For large coupling, correlation of the two fields occurs within a few round trips, before the population inversion has a chance to increase much. However, for small coupling, it takes several hundred round trips for the two lasers' fields to start becoming correlated, so the population inversion has the chance to grow substantially. This in turn will cause the average electric field intensity in the receiver laser to grow. Therefore, the very subtle ($c \approx 0.03$) introduction of the transmitter optical field into the ring of the receiver allows the receiver dynamics enough freedom so that the receiver's population inversion and optical field are still strongly interactive. Then, with the subtle influence of the transmitter optical field, the entire receiver dynamics are *eased* into synchronization much more rapidly than when the transmitter optical field, which has no regard for the receiver population dynamics, is injected dominantly into the receiver cavity.

To finish the examination of the case of identical subsystems, we next determine the minimal value of c which leads to synchronization. In the discussion above the lasers always synchronize, so now we examine weaker coupling yet. To do this we numerically evaluate the largest conditional Lyapunov exponent [4] in much the same way as we find the standard largest Lyapunov exponents in our earlier paper [6]. Now we couple the identical lasers with small coupling c and ask when the largest conditional exponent becomes negative as we vary c. The critical value of coupling was found to be $c_{crit} \approx 1.3\times10^{-3}$. Therefore, for $c < c_{crit}$, we observe no synchronization, as a positive conditional exponent indicates that the synchronization manifold $[\mathcal{E}_T(t)=\mathcal{E}_R(t)]$ is unstable with regard to a dynamical average over the trajectory, and that a typical trajectory in the joint phase space of the two lasers will not asymptotically approach that manifold.

B. Synchronization at $c=1$

We analytically examine our coupled transmitter and receiver system at $c=1$, that is, when we run the receiver open loop. This is the configuration in the Georgia Tech experiments [8,9,17]. In this case the field injected into the receiver is just $\mathcal{E}_T(t)$ and none of the field in the receiver fiber is re-injected into the amplifier. The equations for the two coupled systems are

• For the Transmitter Laser:

$$\mathcal{E}_T(\tau+\tau_R)=\mathbf{M}_{\mathcal{E}}(w_T(\tau),\mathcal{E}_T(\tau)),$$

$$\frac{dw_T(\tau)}{d\tau}=Q-\gamma\{w_T(\tau)+1+|\mathcal{E}_T(\tau)|^2(e^{Gw_T(\tau)}-1)\}; \tag{18}$$

• For the Receiver Laser:

$$\mathcal{E}_R(\tau+\tau_R)=\mathbf{M}_{\mathcal{E}}(w_R(\tau),\mathcal{E}_T(\tau)),$$

$$\frac{dw_R(\tau)}{d\tau}=Q-\gamma\{w_R(\tau)+1+|\mathcal{E}_T(\tau)|^2(e^{Gw_R(\tau)}-1)\}, \tag{19}$$

where $\mathbf{M}_{\mathcal{E}}(w(\tau),\mathcal{E}(\tau))$ is the map defined in earlier sections. Note that in the receiver equations only $\mathcal{E}_T(\tau)$ now appears on the right hand side. Take the difference of the population inversion equations to arrive at

$$\frac{d(w_T(\tau)-w_R(\tau))}{d\tau}$$
$$=-\gamma\{w_T(\tau)-w_R(\tau)+|\mathcal{E}_T(\tau)|^2e^{Gw_R(\tau)}$$
$$\times(e^{G(w_T(\tau)-w_R(\tau))}-1)\}. \tag{20}$$

Noting that $e^x-1\geqslant x$, we can write the following inequality:

$$\frac{d(w_T(\tau)-w_R(\tau))}{d\tau}\leqslant-\gamma(w_T(\tau)-w_R(\tau))$$
$$\times\{1+|\mathcal{E}_T(\tau)|^2e^{Gw_R(\tau)}\}. \tag{21}$$

This shows that $w_T(\tau)-w_R(\tau)$ goes to zero exponentially rapidly at a rate governed by $\gamma(1+|\mathcal{E}_T(\tau)|^2e^{Gw_R(\tau)})$. This result on the synchronization at $c=1$ is a *global* property of these laser systems. Nowhere was a linearization made about the synchronization manifold.

This value of the convergence rate to synchronization agrees within 0.1% of the numerical calculation of the same convergence rate of $w_T(\tau)-w_R(\tau)$ at $c=1$ in our numerical simulations. This gives us additional confidence in both the simulations and in the details of the approximations which went into evaluating the propagation of light around the fiber ring with nonlinear effects [6].

The final step is to use this bounded behavior of the difference in population inversions in the maps

$$\mathcal{E}_T(\tau+\tau_R)=\mathbf{M}_{\mathcal{E}}(w_T(\tau),\mathcal{E}_T(\tau)),$$

$$\mathcal{E}_R(\tau+\tau_R)=\mathbf{M}_{\mathcal{E}}(w_R(\tau),\mathcal{E}_T(\tau)). \tag{22}$$

With this one easily shows that as $w_T(\tau)-w_R(\tau)\to0$ so does $\mathcal{E}_T(\tau)-\mathcal{E}_R(\tau)\to0$. This result demonstrates *global* stability of the synchronization manifold $\mathcal{E}_T(\tau)=\mathcal{E}_R(\tau)$ and $w_T(\tau)=w_R(\tau)$ as it involves no linearization of the equations around this solution. It is the detailed structure of the DFRL equations which permits this demonstration of global stability of the synchronization manifold.

The strong rate of convergence of $w_T(\tau)-w_R(\tau)$, approximately as $\exp(-\gamma|\mathcal{E}_T|^2\tau)$, implies that small perturbations to synchronization which might arise due to noise in the channel or disturbances of the receiver would rapidly be ''cured'' by the auto-synchronization nature of the system at $c=1$. This attractive robustness also suggests that small mismatches in parameters of the transmitter and receiver will also affect the synchronization only slightly. In the next section we show that we indeed have this feature of robust synchronization when we have mismatches in many of the system parameters. An important exception occurs when we have a mismatch in any of the parameters which deal with the complex vectorial nature of the optical field.

C. Mismatched transmitter and receiver

We now examine the influence of system mismatch on synchronization performance. With parameter mismatch, identical synchronization is no longer expected because the transmitter and receiver subsystems themselves are no longer identical. Thus, identically synchronized motion, $\mathcal{E}_T(\tau)=\mathcal{E}_R(\tau)$, is not a solution of the receiver dynamics. However, to communicate via synchronization, we might only need one of the physical observables of the lasers to be in synchronization. For this reason we turn now to an examination of the possibility that only certain measurable properties of the subsystems are synchronized. This phenomenon falls into the broad category of what has been termed *generalized* synchronization [20].

First, we cast generalized synchronization in the language used to discuss identical synchronization. Two subsystems of coupled dynamical systems are usually considered to be in generalized synchronization if there is a comparison function h given by

$$h[g(x),g(y)]=\lim_{T\to\infty}\frac{1}{T}\int_t^{t+T}|H[g(x)]-g(y)|ds \tag{23}$$

that satisfies $||h[g(x),g(y)]||=0$, where $H(\cdot)$ is a smooth, invertible, time-independent function [21–24]. This would imply that if $g(y(t))=H[g(x(t))]$ as $t\to\infty$, then we have generalized synchronization. Examples have been found where generalized synchronization exists, but where H is not an invertible operation [20,25].

To be consistent with the synchronization measure in Eq. (15), we can still use our definition of synchronization with a generalization of the property comparison function on the inside of the integral. For example, to look for generalized intensity synchronization, we define a comparison function

$$H_I[|\mathcal{E}_T(t)|^2,|\mathcal{E}_R(c,t)|^2]=\log_{10}\left(\frac{|\mathcal{E}_R(c,t)|^2}{|\mathcal{E}_T(t)|^2}\right). \tag{24}$$

With the presence of parameter mismatch, the intensities in the two lasers are generally not equal, so the mean value of $H_I(c,t)$ will not necessarily be zero. Therefore, instead of calculating an RMS value, we measure the standard deviation of $H_I(c,t)$ about its mean value over M round trips $\langle H_I(c,t)\rangle_{M\tau_R}$:

$$D_I(c)=\frac{1}{\mathcal{N}_I}\left(\int_{K\tau_R}^{(K+M)\tau_R}[H_I(c,t)-\langle H_I(c,t)\rangle_{M\tau_R}]^2dt\right)^{1/2}. \tag{25}$$

Again this integral is normalized by the factor $\mathcal{N}_I=D_I(c=0)$.

There are other generalized synchronization relationships which could be exploited for specific communication methods. Another possibility would be encoding a message with

polarization modulation [26]. To examine the possibility of generalized polarization synchronization, we introduce a comparison function $H_\theta(c,t)=\theta_S(c,t)$, the angle in Stokes parameter space between the two states of polarization in the two laser subsystems. This leads to a synchronization error measure $D_\theta(c)$, which is completely analogous to $D_I(c)$, calculating the standard deviation of $\theta_S(c,t)$.

Another class of generalized synchronization potentially useful for communications is optical phase synchronization. If the phase of the two lasers is synchronized, communication through phase shift keying (PSK) [26] would be possible. To examine phase synchronization, we introduce the comparison function, $H_\phi(c,t)=\phi_T-\phi_R$, where ϕ_T and ϕ_R are the respective phases of the transmitter and receiver lasers. This leads to another error measure $D_\phi(c)$, again completely analogous to $D_I(c)$ and $D_\theta(c)$, calculating the standard deviation of $H_\phi(c,t)$. Details of the practical calculation of the above synchronization measures are given in the Appendix. Armed with this array of error measures for the various classes of generalized synchronization we now move on to examine the effects of parameter mismatch. As before, we run each laser for $400\,000\tau_R$, couple them with some value of c; $0\leqslant c\leqslant 1$, and calculate the synchronization integrals for $K=20\,000$ and $M=3000$.

The synchronization was found to be extremely robust to mismatches in parameters associated with the active medium of the lasers, namely the gain term G and the pump level Q. Even for 10% mismatches in G and Q, the lasers achieved identical synchronization with errors of around 10^{-3} or 10^{-2}, respectively. The much slower time scale of the active medium makes mismatch of its parameters relatively unimportant, since we have seen that a substantial proportion of the synchronization occurs in the fast time scale.

Accordingly, the effects of mismatches in parameters which correspond to the fast time scale dynamics, i.e., the optical field propagation, are much more detrimental. In the section on identical lasers, we assumed that the optical fields on both lasers evolved the same, i.e., both fibers contained the same birefringence profile and were of identical length, so that the *optical phase* of the two fields can be matched with perfect accuracy. Unfortunately, these are not physically reasonable assumptions. In order to match the optical field polarization evolution and phase of the two lasers, the fiber would have to be in a constant temperature, unstressed environment, the lengths of fiber in both rings would need to match with an accuracy of a fraction of the light's wavelength ($\approx 1.5\ \mu$m), and complete phase stability would have to be achieved between the two lasers.

First we examined synchronization in the presence of optical field polarization evolution mismatch. To model this, we use the fact that the net effect of all fiber birefringence can be represented as an overall Jones matrix $\mathbf{J}_{PC}$. Up to a phase, a completely general Jones matrix can be parametrized by three angles $\theta_1,\theta_2,\theta_3$, so to systematically alter the mismatch in fiber birefringence, we varied the difference of θ_2 between transmitter and receiver.

Figure 6 confirms the detrimental effect on synchronization of a θ_2 mismatch of $\pi/3$. The identical synchronization measure $D_E(c)$ actually becomes worse as coupling increases from zero. At some point the error measure peaks and begins to decline, but it never gets better than the uncoupled case. The generalized synchronization measures $D_\theta(c)$ and $D_\phi(c)$ remain relatively unsynchronized, also. However, the intensity measure $D_I(c)$ does show good synchronization above a certain threshold coupling value. It is worth noting that this threshold corresponds to the error maximum in the identical synchronization measure. In the case of unequal absorptions, using absorption coefficients $R_x=0.45$ and $R_y=0.425$, we find that the behavior is much the same as in the equal absorption case, with a notable similarity being good synchronization values for the generalized intensity synchronization measure. Thus, a polarized light beam possesses similar synchronization behavior to the general-case elliptically polarized light we investigate through this study.

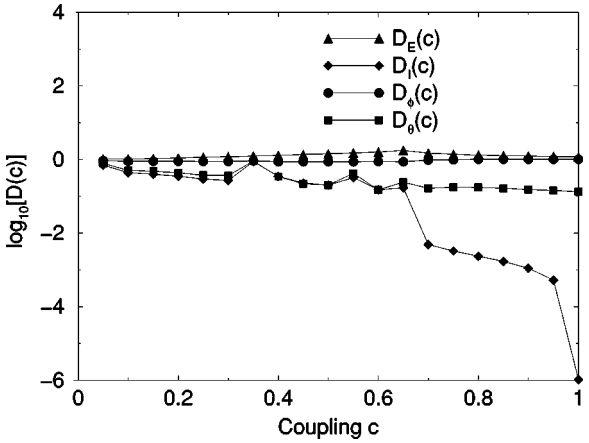

FIG. 6. Synchronization measures for DFRLs with θ_2 mismatch. There is nearly equal absorption, $R_x\approx R_y$ and $\theta_2=\pi/3$. The DFRLs are first coupled for $20\,000\tau_R$ round trips and then the error terms are averaged over an additional $3000\tau_R$.

Looking now at mismatches in the phase between the two lasers, we model a randomly changing phase shift. We consider a phase difference between the two lasers $\Delta\phi(t)$, which begins as some initial phase difference $\Delta\phi(t=0)$, and then on a physically reasonable time scale τ_ϕ [17], is shifted by a random phase amount. We take $\Delta\phi(t+\tau_\phi)=\Delta\phi(t)+\Delta\phi_{random}(\tau_\phi)$, and the coupling between the lasers is modified to be $\mathbf{E}_R'=c\mathbf{E}_T+(1-c)\mathbf{E}_R e^{i\Delta\phi}$. Examining the effect of phase shifts at $\tau_\phi=1\ \mu$s in Fig. 7, we see an orderly gradual progression of the identical synchronization error from order unity for small c to a small error for large c. This simply tells us that the phase mismatch is detrimental, but it has less effect for larger coupling where less of the phase mismatched field from the receiver is being mixed with the field from the transmitter. Looking at the generalized intensity synchronization measures $D_I(c)$ and $D_\theta(c)$, we see that by a coupling of about $c=0.6$ $D_I(c)$ is down to 10^{-2} and $D_\theta(c)$ is down to about 10^{-3} and keeps decreasing from there. Again, even when identical synchronization is not present, there are generally synchronized observables in the optical field.

This type of phase mismatch is commonly cited as the major barrier in achieving ''true'' optical synchronization,

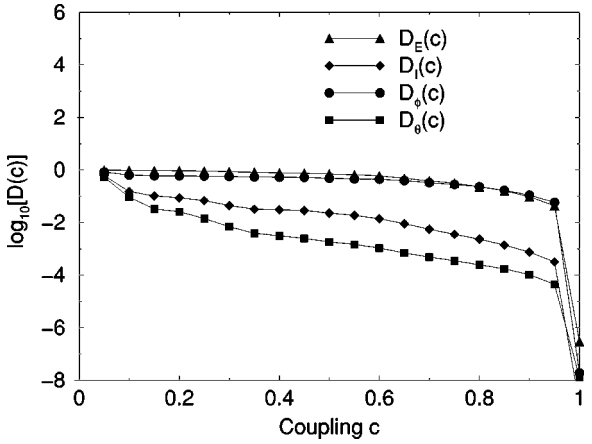

FIG. 7. Synchronization measures plotted against coupling constant c. There is phase mismatch of $\tau_\phi = 1$ μs. The lasers are otherwise identical. The DFRLs are coupled for $20\,000\tau_R$ and the measures are taken over an additional $3000\tau_R$.

i.e., completely synchronized, coupled, entirely optical systems with $c<1$. Therefore, any serious chance for optical synchronization needs to address the physical issue of optical phase mismatch. We suggest the following as a possible line of attack on the problem. In their experimental work at Georgia Tech, VanWiggeren and Roy [9] included an examination of the passive ring structure consisting of two fiber loops of different lengths. When the two loops are rejoined the ring laser dynamics act to optimize the resulting intensity,

$$|(\mathbf{E}_{R1}+\mathbf{E}_{R2})|^2=(|\mathbf{E}_{R1}|^2+|\mathbf{E}_{R2}|^2 + 2|\mathbf{E}_{R1}||\mathbf{E}_{R2}|\cos\theta_R\cos\phi_R), \quad (26)$$

using the same notation as in [9]. Here, θ_R and ϕ_R are, respectively, the angle between the states of polarization and the phase difference between the two optical fields at the point where they are rejoined. The laser acts to optimize the intensity, and the cross term $\cos\theta_R\cos\phi_R$ goes roughly to a maximized value. Therefore, there is a certain amount of phase stabilization occurring due to the optimization effect. We have numerically observed this same cross term maximization. However, in [6] we also reported on a type of frequency filtering which occurs due to the two different times of propagation through the two loops. This type of filtering causes the frequency spectrum to be less broadband and more resembling quasi-periodicity. If the lengths of the loops are as identical as possible, this cross term maximization would exist, but without the frequency filtering. Hence, the advantageous stabilization of the optical phase in the transmitter would still be present, but without paying the penalty of frequency filtering. Perhaps experimental work in the future will examine this idea further.

We end by mentioning that with substantial mismatches in the lengths of fiber in the two lasers, all synchronization was completely obliterated. However, this result is not surprising. Once the lasers are coupled, the resulting field is propagated around the ring of the receiver and meets up with the incoming field from the transmitter to be coupled and propagated once more. If the length mismatch is severe enough, the receiver's complex envelope will not match up with the incoming complex envelope from the transmitter, and there is no reason to expect that there would be any synchronization, since spatial envelope dynamics are only very weakly correlated through the population inversion and the fiber effects.

D. Noise in the communications channel

Two physical lasers will not have identical operating parameters, and synchronization of two physical lasers will unavoidably be subjected to the parameter mismatches just discussed. Another unavoidable issue is the effect on synchronization of noise in the channel by which the two lasers are coupled. Any physical application of synchronizing DFRLs will invariably be effected by this noise, so we examine that case here.

We consider signal to noise ratios 0 dB and 40 dB. We concentrate on the case of two lasers with identical parameter values which are coupled via a noisy fiber channel. The average noise amplitude $\langle|\xi|\rangle$ we use is determined from the signal-to-noise ratio (SNR) given by

$$\mathrm{SNR}=20\log_{10}\frac{\langle|\mathcal{E}_T|\rangle}{\langle|\xi|\rangle} \quad (27)$$

Noise was added to the field arriving from the transmitter before coupling. Instead of receiving as input $c\mathcal{E}_T+(1-c)\mathcal{E}_R$, the receiver now receives the modified noisy input given by $c\mathcal{N}_\xi(\mathcal{E}_T+\zeta)+(1-c)\mathcal{E}_R$, where ζ is a complex polarization noise two-vector. The components of ζ are random Gaussian-distributed numbers with unit variance, multiplied by the average noise amplitude $\langle|\xi|\rangle$. The normalization on the incoming transmitter field plus noise is chosen so that the variance of this incoming ''noisy'' signal $\mathcal{N}_\xi(\mathcal{E}_T+\zeta)$ was equal to that of the clean transmitter field $\mathcal{E}_T$:

$$\mathcal{N}_\xi=\frac{\langle|\mathcal{E}_T|\rangle}{\sqrt{\langle|\mathcal{E}_T|\rangle^2+\langle|\xi|\rangle^2}}. \quad (28)$$

Again the lasers were allowed to couple for $20\,000\tau_R$ and then the error value $D_E(c)$ was averaged over the next $3000\tau_R$.

Looking first at $D_E(c)$ for identical lasers in Fig. 8, we see that due to the noise there is a steady growth in the synchronization error as coupling is increased. Even for a SNR of 0 dB, at small coupling $c\leqslant 0.1$, we have below a 10% normalized RMS error. However, for large coupling constants, the 0 dB SNR value leads to synchronization errors of 20% and more. For SNR of 40 dB, we see that for all coupling constants the RMS error is well below a few parts in 1000. Here it is obvious that the rate of growth of the normalized RMS error as a function of coupling constant is very much the same for the range of SNR values. The SNR we quote is the channel signal-to-noise ratio, while the noise entering the receiver is $c\zeta$ when we feedback $(1-c)$ of $\mathcal{E}_R$, thus the effective signal-to-noise ratio in the receiver is higher when c increases from zero.

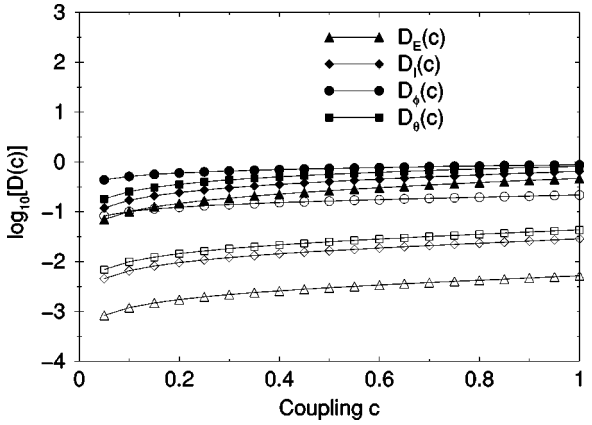

FIG. 8. Synchronization errors for identical DFRLs with channel noise. The filled symbols represent SNR=0 dB and the clear symbols SNR=40 dB. The DFRLs are first coupled for $20\,000\tau_R$ and then the error terms are averaged over an additional $3000\tau_R$.

All the generalized synchronization measures in Fig. 8 show rather much the same behavior as the identical synchronization case. For high SNRs, the synchronization is good for all measures (except the phase synchronization measure), and all measures continue to show a preference for weaker coupling, a type of nonlinear noise reduction. In optical fiber systems, channel noise is extremely low, and is usually not a concern. Our purpose here is to also examine what substantial noise, say due to multi-user communications in the background, might do to our synchronization. It is encouraging that the lasers actually synchronize better for weaker coupling in the presence of noise, as this might be a clue as to how to utilize multiple channels for chaotic laser communication. This fact matches well with our earlier observation that the most rapid convergence of the two lasers into synchronization also occurs at extremely low coupling. These two facts can perhaps combine in a useful way later when examining communication methods more closely.

E. Alternate coupling scheme

The detrimental effects of the optical field parameter mismatches lead us to propose another way to synchronize the lasers without coupling the full optical field of the transmitter laser into the fiber ring of the receiver laser. We briefly examine a synchronization scheme where the electric field intensity of the transmitter laser is detected, and used to electro-optically modulate the optical *intensity* in the receiver laser in an effort to drive the receiver into a state of generalized intensity synchronization.

In Fig. 9 the proposed intensity synchronization strategy is diagrammed. This scheme is close to the previous optical amplitude coupling strategy, except that we now insert an electro-optical intensity modulator. The electro-optic modulator uses the incoming electric field to destructively interfere with itself, thereby lowering the total intensity of the incoming state. Technically, it can do this in various ways [27], but we chose to simulate a Mach-Zehnder waveguide modulator [14,27]. The important result is that the amount of phase shift between the two channels in the receiver Ψ_R is

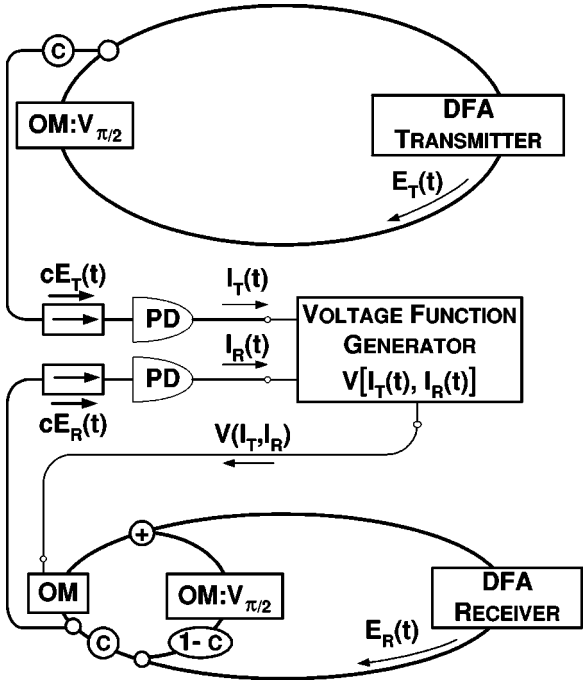

FIG. 9. Diagram of optical modulation coupling scheme. All optical modulators (OM) are biased to a voltage of $V_{\pi/2}$. The optical fields of the transmitter and receiver are detected by photodiodes (PD) and fed into a voltage function generator. This voltage is then used to electro-optically modulate the *c* branch of the receiver's ring to bring the receiver DFRL into a state of generalized intensity synchronization with the transmitter DRFL's intensity.

linearly proportional to the voltage applied across the electro-optic crystal. We write this phase shift following the conventions in [14] as

$$\Psi_R = \pi \frac{V}{V_\pi} \tag{29}$$

where V_π is the voltage needed to create a phase shift of magnitude π. The net effect on the incoming intensity is

$$|\mathcal{E}'_R(t)|^2 = \cos^2\left(\frac{\Psi_R}{2}\right)|\mathcal{E}_R(t)|^2, \tag{30}$$

where the primed (unprimed) field corresponds to the field after (before) the electro-optic modulator. This configuration only allows for modulation to a lesser intensity if the unmodulated state is $V=0$. For this reason we bias the modulator with a voltage of $V_{\pi/2}=V_\pi/2$ which gives a constant phase shift of $\Psi_T=\pi/2$. We now place an identical bias in the transmitter to make the lasers identical again, and synchronization conditions are favorable.

To synchronize, we detect the incoming transmitter electric field with a photodiode to create a current proportional to $|\mathcal{E}_T|^2$. Meanwhile, the receiver intensity is detected before the modulator by another photodiode and a current proportional to $|\mathcal{E}_R|^2$ is also created. These currents are input into a voltage function generator which outputs a voltage to the electro-optic modulator. We note here the considerable

physical task required as all these propagation times must be matched appropriately. Here we assume that we can physically create the ideal voltage function:

$$V(|\mathcal{E}_T(t)|^2,|\mathcal{E}_R(t)|^2)=\frac{2V_\pi}{\pi}\cos^{-1}\left(\frac{|\mathcal{E}_T(t)|}{\sqrt{2}|\mathcal{E}_R(t)|}\right). \quad (31)$$

Using this phase shift in Eq. (30), we see that we immediately arrive at intensity synchronization, because

$$|\mathcal{E}'_R(t)|^2=\cos^2\left(\cos^{-1}\left[\frac{|\mathcal{E}_T(t)|}{\sqrt{2}|\mathcal{E}_R(t)|}\right]\right)|\mathcal{E}_R(t)|^2=\tfrac{1}{2}|\mathcal{E}_T(t)|^2, \quad (32)$$

which is exactly equal the optical intensity in the transmitter after it has proceeded through its biased modulator. Note that we cannot allow voltage functions where $|\mathcal{E}_T(t)|^2 > 2|\mathcal{E}_R(t)|^2$ because then the arc cosine argument will be greater than one. Therefore we limit the voltage at that point.

We also allow for a variation of coupling constants by splitting the receiver ring into two branches in the proportion $c:(1-c)$. The branch $c\mathcal{E}_R$ then goes through the electro-optic modulator, and the $(1-c)\mathcal{E}_R$ diverts around the modulator and is subjected to a 50% intensity attenuation. The two branches are then joined again before entering the DFA.

The results are shown in Fig. 10. Since only the intensity is synchronized, there is no sign of identical, phase or polarization synchronization. However, we see that for larger c, there is generalized intensity synchronization within 10^{-2}. These synchronization values are in the same range as the intensity synchronization achieved in the optical coupling in the presence of polarization evolution and phase mismatches. In the next section, we will attempt to communicate with this configuration and discover whether or not intensity synchronization with errors of order 10^{-2} is good enough for reliable message recovery.

Relatively successful generalized intensity synchronization seems to be achievable through optical modulator coupling. However, there are some unanswered questions. One is that the photodiodes which detect the intensities have finite bandwidths (up to the order of GHz). The question is whether the lasers synchronize with just lower frequency information being shared from transmitter to receiver. Also, what are the possibilities for a function of the form $V(|\mathcal{E}_T|^2,|\mathcal{E}_R|^2)$? Are there physically high-speed functions which maximize the efficiency of the synchronization? These and other questions will be the focus of further study.

IV. COMMUNICATIONS

We now attempt transmission and recovery of a bit string using an electro-optically modulated amplitude shift keying (ASK) technique for identical lasers with optical coupling and with coupling by electro-optic modulation. This is the main method employed in the experimental cases by Roy and VanWiggeren [8,9,17]. The setup is shown schematically in Fig. 11.

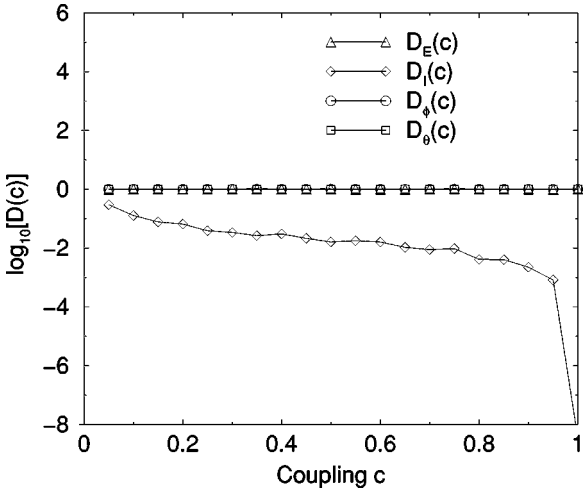

FIG. 10. Synchronization errors for identical DFRLs with coupling by an optical modulator. The DFRLs are first coupled for $20\,000\tau_R$ and then the error terms are averaged over an additional $3000\tau_R$.

An electro-optical modulator is added to the transmitter ring in order to electro-optically modulate the bit string onto the chaotic optical waveform in the transmitter. In order to keep the mean round-trip optical intensity as close to constant as possible (to maintain stability) we modulate the intensity by $|\mathcal{E}_T(t+1)|^2=m^2(t)|\mathcal{E}_T(t)|^2$, where $m=\sqrt{1+K}$ for a ''1'' bit, and $m=\sqrt{1-K}$ for a ''0'' bit. Also, in the transmitter, before the intensity is modulated, we split the optical field in a proportion $c:(1-c)$. The branch corresponding to the c value is electro-optically modulated, and the $(1-c)$ branch is not modulated. Before the two branches are rejoined, the modulated field is coupled out of the c branch and sent off to the receiver. This is necessary to keep the optical field equations in exact synchronization for all c as they enter their respective active media. For $c=1$, the unmodulated branch is not needed (as was experimentally shown in [8,9,17]), but for $c\neq 1$ synchronization will be lost. It is for this reason that we introduce this idea of partial modulation of the transmitter intensity. Note in Fig. 11 that if the unmodulated branch were not present, the optical fields entering the active media would not be equal. With the branch, the optical field entering the active medium of the transmitter is $(cm(t)+1-c)\mathcal{E}_T(t)$ while the field entering the receiver is $cm(t)\mathcal{E}_T(t)+(1-c)\mathcal{E}_R(t)$. So for the synchronized case, where $\mathcal{E}_T(t)=\mathcal{E}_R(t)$, the active media see identical incident optical fields, regardless of the modulation $m(t)$ for $c<1$. Of course, the question of stability of synchronization remains. We note here that the chosen bit rate attempted in this study is a randomly chosen rate which is suitable for the current purposes. We have not undertaken a study of optimizing the bit rate nor claim that the used bit rate *is* optimal with regard to the time scales of the lasers or the chaotic dynamics.

A. Identical lasers with optical coupling

We take this dual EDRFL system and transmit a message. We choose a non-return-to-zero bit rate of 1 GHz, corre-

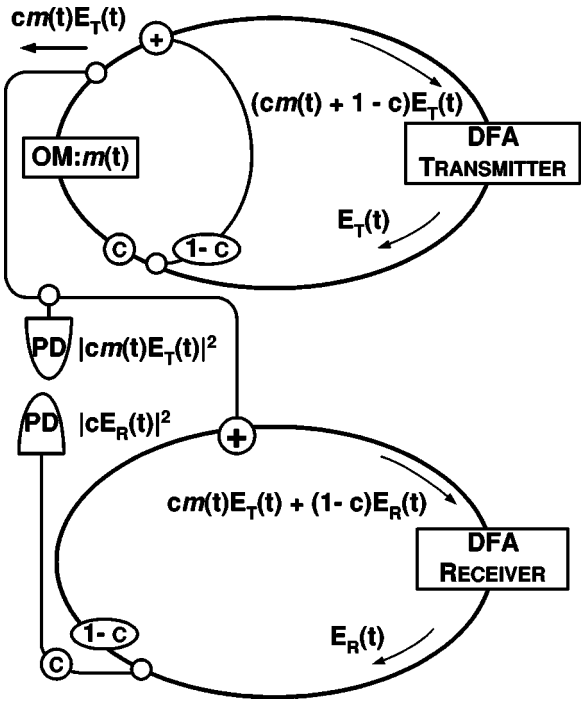

FIG. 11. Diagram of communications using optical coupling scheme. The setup is almost identical to Fig. 2 except it contains an additional $c:1-c$ branch in the transmitter. This branch must be included if synchronization is to be achieved for couplings in the range $0<c<1$. Note for $\mathcal{E}_T(t)=\mathcal{E}_R(t)$, the optical fields entering both active mediums are identical, even with the presence of modulation.

sponding to 13 model integration iteration time steps per bit. To recover the bits at the receiver, the incoming intensity from the transmitter is detected by a photodiode and produces a current proportional to the value $|cm(t)\mathcal{E}_T(t)|^2$ (see Fig. 11). We simultaneously couple out the optical field from the receiver ring with a $c:(1-c)$ coupler and detect the value $|c\mathcal{E}_R(t)|^2$ with another photodiode. If $\mathcal{E}_T(t)=\mathcal{E}_R(t)=\mathcal{E}(t)$, the transmitter's intensity divided by the receiver's intensity will recover the message, $m^2(t)$. The overall decision on a ''0'' bit or a ''1'' bit is made over all N time steps within the bit time period by averaging the received message $m^2(t)$ over the N time steps and using a decision threshold value of $\langle m^2(t)\rangle_N=1$.

We transmit 10^7 independent random bits and record the bit error rate (BER). If no errors occur, we report a BER of zero, noting that this is only true up to the first 10^7 bits sent. For couplings in the range $0.005\leqslant c\leqslant 1.0$, we obtained error-free recovery of the whole bit string. This is consistent with the above conjecture that the partial modulation coupling scheme will not lose synchronization with the addition of intensity modulation. If synchronization is not being effected, one could further conjecture that errors will never arise in the long term state since synchronization will continue to be just as robust. No claim of proof of this fact is made here, as it is conceivable that for sufficiently deep modulation stability properties could change.

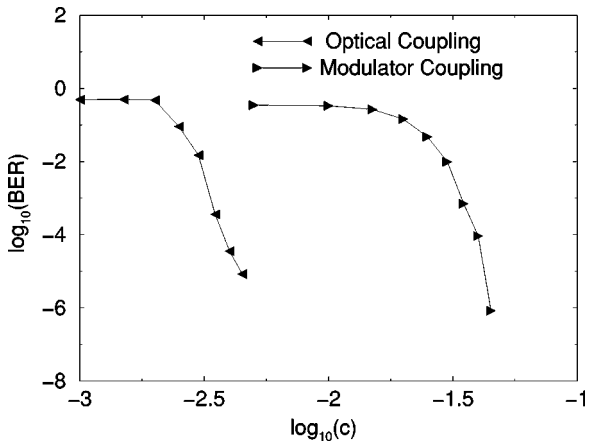

FIG. 12. Bit error rate versus coupling for the case of identical lasers using the two different coupling schemes. The coupling range is $0.0\leqslant c\leqslant 0.06$. The encoding is done via ASK modulation at a bit rate of 1 GHz with modulation factor $K=0.1$.

We turn to a search of the minimum error-free coupling strength. In Fig. 12 we see that we begin to get nonzero BERs below a critical coupling of $c_{crit}=5.0\times10^{-3}$. The error-free recovery of bits for such small couplings is remarkable. The coupling scheme practically guarantees this since the lasers synchronize at such small coupling strengths to begin with. We note a small difference in the critical coupling found for straight synchronization in the previous section ($c_{crit}=1.3\times10^{-3}$), and the critical coupling for communications ($c_{crit}=5.0\times10^{-3}$). It is possible that the electro-optic modulation actually increases the largest Lyapunov exponent in the rings [found above to be approximately $(6.3\pm0.3)\times10^3\,\mathrm{s}^{-1}$ without electro-optic modulation] which would then increase the largest conditional Lyapunov exponent, and thereby raise the value of the critical coupling needed from the simple synchronization level to the calculated level of necessary coupling strength needed for synchronization in the communications case.

To complete the bit error rate calculations, we include the performance of the optically coupled system when faced with communication channel noise. In Fig. 13 we plot the BER versus coupling for SNRs in the range 20 dB to 60 dB. We see that for a SNR of 20 dB, there is no message recovery. In this case, the variance of the channel noise is equal to the modulation amount ($K=0.1$) so lack of recovery is not surprising. We see an improvement at a SNR of 40 dB, where a range of lower coupling values are preferred. This improvement is accentuated at a SNR of 60 dB where the BER = 0 (up to 10^7 bits) for couplings in the range $0.1\leqslant c\leqslant 0.4$, while with increasing coupling we get BERs on the order of 10^{-2} as $c\to1$. These results further confirm the previous indications that for optically communicating with the method here described, better success may be achieved by using coupling strengths much less than $c=1$.

B. Identical lasers with coupling by electro-optic modulation

We next modify our transmission scheme in the spirit of our alternative method of coupling by electro-optic modula-

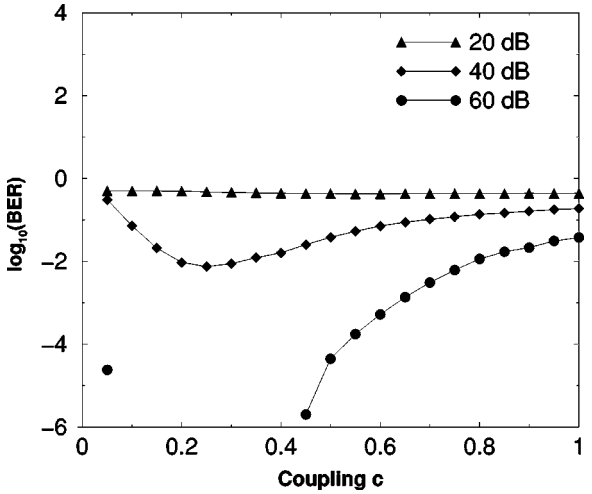

FIG. 13. Bit error rate versus coupling for the case of optically coupled identical lasers in the presence of communication channel noise. The encoding is done via ASK modulation at a bit rate of 1 GHz with a modulation factor of $K=0.1$.

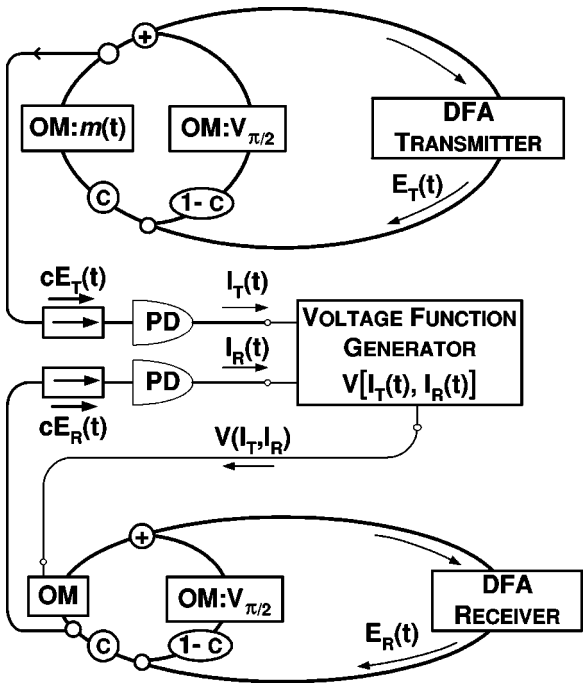

FIG. 14. Diagram of communications using optical modulation coupling scheme. Again, the scheme is almost identical to Fig. 9 except for the presence of a $c:1-c$ branching in the transmitter. Again, this is added in an attempt to achieve synchronization in the presence of modulation for couplings in the range $0<c<1$.

tion. The setup is similar to the above optical coupling setup except we now include an identical $c:(1-c)$ fiber branching in the receiver laser which is identical to the one in the transmitter laser (Fig. 14). Recall that we previously found that the only robust synchronization in this method of coupling was generalized intensity synchronization. So this examination serves as a test of whether or not ASK is feasible with only intensity synchronization present.

Unlike the optical coupling method above we do not need to make special provisions to recover the incoming encoded message. The recovery method is already in place. Once the lasers are synchronized, the voltage function generator will be putting out a relatively constant voltage of $V_\pi/2$. Once the message starts arriving, this voltage function will respond in a manner to retain synchronization. If a ''1'' bit is transmitted, then the incoming intensity value $|cm(t)\mathcal{E}_T(t)|^2$ will cause the voltage function generator to decrease its voltage (thereby decreasing the phase shift and raising the receiver's intensity). A likewise voltage increase will occur if a ''0'' bit is transmitted. Therefore we can just monitor the voltage and average over the N time steps within the bit time period as using a value of $\langle V\rangle_N = V_\pi$ as a decision threshold.

Again we send 10^7 random bits and calculate appropriate BER plots. We found that the BER was more sensitive to the modulation amount value K that in the optical coupling case. This is likely due to the less robust synchronization of this method compared to the optical coupling method. By roughly optimizing the modulation amount value in the range $0.01\leqslant K\leqslant 0.1$ for coupling strengths in the range $0.05\leqslant c\leqslant 1.0$, we were able to achieve error-free recovery (again noting that this is only accurate up to the first 10^7 bits). The existence of generalized intensity synchronization is sufficient for suitable ASK message recovery.

Again we search for the critical minimum coupling strength for error-free transmission in Fig. 12 for coupling strengths in the range $0.0\leqslant c\leqslant 0.05$. Here we do see a critical coupling an order of magnitude higher than the optical coupling case, even with the optimizing of the modulation amount K. The critical coupling strength appears to be $c_{crit}\approx 4.5\times 10^{-2}$. This higher critical coupling strength is again likely due to the fact that the generalized intensity synchronization error is more robust in identical lasers with optical coupling than in identical lasers with coupling by electro-optic modulation. However, the scheme has the potential for much improvement and will be the subject of further detailed study.

V. CONCLUSIONS AND DISCUSSION

We began with a study of the quality of synchronization when all the parameters of the transmitter and receiver lasers were identically matched. Synchronization occurred for coupling strengths down to $c_{crit}=1.3\times 10^{-3}$. For strong coupling ($c\to 1$), we found that synchronization sets in essentially instantaneously ($\tau_S\leqslant 1$ μs). We also found evidence of two distinct synchronization time scales. There is an immediate jump towards synchronization due to the initial mixing of the optical fields, after which a second rate of convergence takes over due to the asymptotic relaxation of the population inversion in the active medium to its equilibrium value. We numerically showed that this second convergence rate has a maximum in the coupling range $0.02\leqslant c\leqslant 0.04$, and decreases to a minimum rate at $c=1$. We analytically demonstrated the global stability of the synchronization manifold at $c=1$, and also determined a lower bound on the magnitude of the convergence rate.

We then turned to the examination of the effect of param-

eter mismatch between the two laser subsystems. We found that while the synchronization dynamics was relatively robust against mismatches in the physical parameters of the two lasers, any mismatch in the optical field propagation (either phase or polarization mismatch) critically effected the synchronization. The effect of noise in the communications channel was also examined, and we found that the lasers actually synchronized better for lower coupling. This indicated that a sort of nonlinear noise reduction was occurring via the coupling scheme, and hinted towards some possible applications in regards to multi-user communications. An alternate method of coupling the lasers was examined which was created in an attempt to bypass all of the synchronization problems found regarding the optical field phase and state of polarization mismatches. Intensity synchronization on the order of that observed in the optical coupling cases was observed.

Finally, an ASK modulation scheme was used to modulate a message onto the intensity of the chaotic waveform in the transmitter to be recovered at the receiver. For a pair of identical lasers coupled both by direct optical coupling and the alternative coupling-by-intensity modulation method, remarkable bit error rates were achieved. There was error-free recovery of bits (10^7 bits were sent) down to a coupling strength of $c_{crit}=5.0\times10^{-3}$.

There are several directions in which one may pursue the work reported here. A straightforward possibility is the consideration of other rare-earth-doped fibers where T_1 is shorter. With Pr or Nd one can achieve T_1's as small as 100 μs, and this would change many of the features we have reported. It is likely that the sensitivity of synchronization to polarization or phase mismatches would remain, but while sacrificing synchronization for such small values of c, we may accomplish other goals such as smaller bit error rates in the presence of channel noise associated with larger conditional Lyapunov exponents on the synchronization manifold. Another direction would be to replace the active element in the ring lasers with other devices, and semiconductor lasers immediately suggest themselves. With these $T_1\approx1$ ns, and many of the operating characteristics investigated here change. We shall report on an investigation of this class of chaotic transmitter and receiver [28].

ACKNOWLEDGMENTS

We thank the members of INLS, Alistair Mees, and Ulrich Parlitz for helpful discussions on this subject. This work was part of a joint UCSD/Georgia Tech/Cornell effort, and we are grateful to Steve Strogatz, Raj Roy, Govind Agrawal, and others in that program for detailed discussions of the issues here. This work was supported in part by the U.S. Department of Energy, Office of Basic Energy Sciences, Division of Engineering and Geosciences, under Grant No. DE-FG03-90ER14138, in part by National Science Foundation Grant No. NCR-9612250, and in part by the Army Research Office, DAAG55-98-1-0269, MURI Project in Chaotic Communication.

APPENDIX: GENERALIZED SYNCHRONIZATION MEASURES

Here, we provide the details behind the calculation of two of the generalized synchronization measures used in the paper. To examine the possibility of generalized polarization synchronization, we introduced a new comparison function

$$H_\theta(c,t)=\theta_S(c,t), \tag{A1}$$

where $\theta_S(c,t)$ is the angle in Stokes parameter space between the two states of polarization in the two laser subsystems. θ_S is found using the Stokes parameters [26]

$$S_0=a^2+b^2+c^2+d^2, \tag{A2}$$

$$S_1=a^2+b^2-c^2-d^2, \tag{A3}$$

$$S_2=2(ac+bd), \tag{A4}$$

$$S_3=2(ad-bc), \tag{A5}$$

for an electric field with arbitrary x and y polarization

$$\mathcal{E}=(a+ib)\hat{x}+(c+id)\hat{y}. \tag{A6}$$

These satisfy

$$S_0^2=S_1^2+S_2^2+S_3^2, \tag{A7}$$

so the state of polarization can be represented as a vector $\vec{S}$ in (S_1,S_2,S_3) space of magnitude S_0. The angle between the two states of polarization of $\mathcal{E}_T$ and $\mathcal{E}_R$ is then

$$\theta_S=\cos^{-1}\left[\frac{\vec{S}_T\cdot\vec{S}_R}{S_{0_T}S_{0_R}}\right]. \tag{A8}$$

This is the value which is time averaged to examine if the lasers are in a state of generalized polarization synchronization.

Also, to look for phase synchronization, we introduced the comparison function,

$$H_\phi(c,t)=\phi_T-\phi_R\,. \tag{A9}$$

Each electric field $\mathcal{E}_T$ and $\mathcal{E}_R$ is in general elliptically polarized. We desire to quantify the phase with respect to its own

polarization basis, so we define the phase of the electric field as its phase in the x-y laboratory frame minus the angle of the major axis of the polarization ellipse with respect to the x-y laboratory frame, i.e.,

$$\phi = \phi_{xy} - \Phi_{ellipse} \pmod{\pi}, \tag{A10}$$

where, using the above definitions, we have

$$\phi_{xy} = \tan^{-1}\left[\frac{c}{a}\right] \tag{A11}$$

and

$$\Phi_{ellipse} = \frac{1}{2}\tan^{-1}\left[\frac{S_2}{S_1}\right]. \tag{A12}$$

[1] H. Fujisaka and T. Yamada, Prog. Theor. Phys. **69**, 32 (1983).
[2] V.S. Afraimovich, N.N. Veirchev, and M.I. Rabinovich, Izv. Vyssh. Uchebn. Zoved. Radiofiz. **29**, 795 (1986).
[3] D. Hansel and H. Sompolinsky, Phys. Rev. Lett. **68**, 718 (1991).
[4] L.M. Pecora and T.L. Carroll, Phys. Rev. Lett. **64**, 821 (1990).
[5] See the papers in the special issue of IEEE Trans. Circuits Syst. I: Fundam. Theory Appl. **44** (10), edited by M. P. Kennedy and M. Ogorzalek, 1997.
[6] H.D.I. Abarbanel, M.B. Kennel, M. Buhl, and C.T. Lewis, Phys. Rev. A **60**, 2360 (1999).
[7] H.D.I. Abarbanel and M.B. Kennel, Phys. Rev. Lett. **80**, 3153 (1998).
[8] R. Roy and G. VanWiggeren, Science **279**, 1198 (1998).
[9] G. VanWiggeren and R. Roy, Phys. Rev. Lett. **81**, 3547 (1999).
[10] N.F. Rulkov and A. Volkovskii, Tech. Phys. Lett. **19**, 97 (1993).
[11] L. Kocarev and U. Parlitz, Phys. Rev. Lett. **74**, 5028 (1995).
[12] M.M. Sushchik, N.F. Rulkov, L. Larson, L.Sh. Tsimring, H.D.I. Abarbanel, and K. Yao, IEEE Commun Lett. **4**, 128 (2000).
[13] Q.L. Williams, J. Garcia-Ojalvo, and R. Roy, Phys. Rev. A **55**, 2376 (1997).
[14] A. Yariv, *Optical Electronics* (CBS College, 1985).
[15] G. P. Agrawal, *Nonlinear Fiber Optics*, 2nd ed. (Academic P, San Diego, 1995).
[16] C.D. Poole and R.E. Wagner, Electron. Lett. **22**, 1029 (1986).
[17] R. Roy. and G. VanWiggeren (private communication).
[18] L. Luo, T.J. Lee, and P.L. Chu, J. Opt. Soc. Am. B **15**, 972 (1998).
[19] R. Brown and L. Kocarev, Chaos **10**, 344 (2000).
[20] N.F. Rulkov, M.M. Sushchik, L.S. Tsimring, and H.D.I. Abarbanel, Phys. Rev. E **51**, 980 (1995).
[21] L. Kocarev and U. Parlitz, Phys. Rev. Lett. **76**, 1816 (1996).
[22] U. Parlitz, L. Junge, and L. Kocarev, Phys. Rev. Lett. **79**, 3158 (1997).
[23] B.R. Hunt, E. Ott, and J.A. Yorke, Phys. Rev. E **55**, 4029 (1997).
[24] R. Brown, Phys. Rev. Lett. **81**, 4835 (1998).
[25] N.F. Rulkov and M.M. Sushchik, Phys. Lett. A **214**, 145 (1996).
[26] S. Betti, G. DeMarchis, and E. Iannone, *Coherent Optical Communications Systems* (Wiley, New York, 1995).
[27] S.H. Chuang, *Physics of Optoelectric Devices* (Wiley, New York, 1995).
[28] H.D.I. Abarbanel, M.B. Kennel, L. Illing, and C.T. Lewis (unpublished).